3rd URSI AT-AP-RASC, Gran Canaria, 29 May – 3 June 2022

Classification based Detection of Geomagnetic Storms using LSTM Neural Network

Ishita Gulati*[(1)], Handong Li[(1)], Martin Johnston[(1)], and Satnam Dlay[(1)]
(1) Newcastle University, United Kingdom, i.gulati2@ncl.ac.uk

Abstract

Solar activity influences near-Earth space phenomena by releasing solar flares, high speed solar wind, and CMEs which tend to give rise to geomagnetic storms. They affect the Earth's magnetic field and upper atmosphere by interfering with the radio signals sent from space and hinder GNSS technology that relies on the accuracy of these signals. If information about the onset of the storms is available even a few hours prior to the actual storm, it can help in estimating the economic and global financial losses that ensue because of them. A large percentage of our daily work relies on accurate positioning, navigation and timing. Promising results have been achieved in the recent years for predicting *Dst* by using artificial neural networks. In this paper, a neural network technique called the LSTM is designed which recognises numerical time series data. An algorithm that detects the *Dst*, an hourly measure of the ring current in the form of time series data, using other geomagnetic indices has been proposed. Preliminary results exhibit a positive response to the classification based detection technique used in this paper.

1 Introduction

Solar activity driven by the solar magnetic field, is released from the Sun in the form of bursts of electromagnetic radiation (flares), CMEs and SEPs. When remains of this solar activity reach the Earth, they derange the Earth's magnetic field, inducing geomagnetic storms. Some of these storms are strong enough to interfere with the GNSS signals sent from space and debilitate technical operations related to it on Earth. Table 1 shows that the number of minor storms significantly increased from 0% in 1996-2008 to 62% in 2008-2017. Major and sever storms did not record that spike but, overall, the seasonal distribution of geomagnetic storms increased from 44% in SC-23 to 54% in SC-24 along with the occurrence rate from 2003 to 2015 [1]. This implies that we are constantly vulnerable to either type of geomagnetic activity. Previous studies have proven that some of these storms disabled communication and navigation services in different parts of the world and even caused damage to the functioning of satellites orbiting in space. Since our dependency on GNSS has increased multi-fold in the last few years, loss of signal for a few minutes also becomes unaffordable for safety critical, liability-critical and non-critical applications.

Space weather is a phenomena that cannot be ceased and predicting solar storms is something that still needs to be achieved in totality. With recent advancements in machine learning and neural networks, this now seems feasible. LSTM has been chosen for his study as it is best known for solving time-series problems and achieving prediction-based anomaly detection. Prediction is highly dependent on the reliable detection which can then be used for the classification of geomagnetic storms.

Table 1. Percentage Occurrence of Geomagnetic Storms

	1996-2008	2008-2017
Minor	0%	62%
Major	56%	34%
Severe	44%	4%

1.1 Space Weather and Neural Networks

To characterise equatorial magnetic variations used for describing geomagnetic activity, space weather experts have been using the Disturbance Storm Time (*Dst*) index which is expressed in nanoTesla (nT). It is measured by computing the hourly H-component magnetic variations which show the show the effect of the globally symmetrical westward flowing high altitude equatorial ring current. Depending on the depth of depressions in the *Dst*, the storm phases are classified as sudden storm commencement, main phase and recovery phase. Thus, detecting and/or forecasting *Dst* is critical to GNSS operation.

Use of neural networks in GNSS related operations evolved from the twentieth century when [2] used a linear filtering prediction method to connect *Dst* and B_z; [3] used Elman recurrent NNs to predict *Dst* 1-8 hours in advance from the solar wind alone and [4] developed forecast models for K_p and Dst. From being able to use a single feature to predict one parameter, the studies advanced to using a variety of solar data indices to predict multiple parameters such as done by [5], who used ANNs and Boyle index to predict K_p, Dst and AE; use of NARMAX methodology based on a non-linear network to minimise error by [6] and swarm particles optimization by [7]. Most recent contributions on *Dst* prediction include using GP-AR and GP-ARX models that generate predictive distributions of *Dst* by [8] and a combination of LSTM and Gaussian process, which has been referred to as GPNN by [9]. Their model worked well for 1-3 hr ahead forecast but also overestimated during super storms. [10] trained an ANN with magnetic data

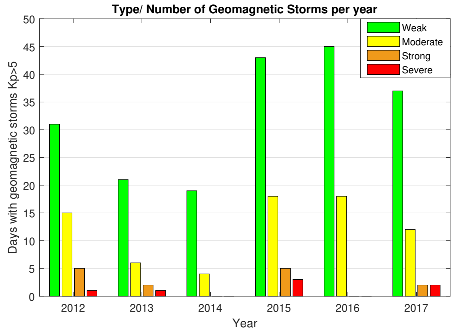

Figure 1. Geomagnetic storm classification and occurrence

from SWARM satellite to compute *Dst*. Their model gave a 'good estimate' for disturbed state of the ionosphere but overestimated during low-moderate geomagnetic activity.

LSTM is one of the most powerful subset of artificial RNNs as they are peculiarly convenient while classifying and making predictions on time-based data. Due to this reason, this study has been based on training time series data of Earth's magnetic field using the LSTM network to further classify and detect geomagnetic storm onsets. The use of solar data has been proven to be useful to train the model as shown in [11]. The novelty of this paper lies in using classification based detection anomaly. This model classifies the storms based on their intensity and then predicts its future *Dst* state as explained in the below sections.

2 Storm classification and Hyper parameters

Based on the magnitude of *Dst* index, the geomagnetic storms are classified as either 'weak/no storm' (G1, $\leq$-50nT), 'moderate storm' (G2, $\leq$-100nT), 'strong storm (G3, $\leq$-200nT) or 'severe storm' (G4, $\leq$-350nT) [12]. Fig. 1 shows the number of geomagnetic storms that occurred in the period 2012-2017 classified on the basis of their strength based on NOAA scales. The reason for selecting these years is the reliable data availability and the fact that 40 of top 50 geomagnetic storms of solar cycle 24 occurred in this period.

3 Data and Methodology

The dataset includes Geocentric Solar Ecliptic (GSE) magnetic field data comprising of magnitude of the IMF (nT), B_x (nT), B_z (nT); plasma proton density (N/cm^3); Auroral Electroject (*AE*) index (nT) and proton flux over 10 MeV (also known as network features). This is converted to the 'Ground-Truth dataset' (using MATLAB) by adding labels to four classes (weak/moderate/strong/severe) on the basis of the *Dst*. To develop the network, the GT-dataset is split into training dataset (2012-2016) based on which the model learns, and the testing dataset (2017) which is used to detect *Dst*.To create an LSTM network for sequence-to-label classification, a classification output layer is added to the existing system.

4 LSTM model architecture

The LSTM model used in this study consists of a sequence input layer. The size of this layer equals the number of features of the input data which are shuffled after every epoch within a batch to minimize the computation burden. This allows to reduce the randomness of the network and not proceed towards descent. It is followed by a single LSTM layer with 500 HU and a hyperbolic tangent activation function. This layer is then succeeded by the fully connected layer whose size equals the number of classes. The network ends with a softmax layer and a classification output layer. This classification output layer classifies the data based on the GT-dataset. To ensure the process of training within a confidence level, hyperparameters of the LSTM network must be calibrated or manually optimised. These have been listed in Table 2.

Table 2. LSTM Hyperparameters

Hyperparameters	Value
Optimizer	'Adam'
Hardware resource	Single CPU
Learning rate	0.001
Gradient threshold	2
Gradient threshold method	'l2norm'
Sequence length	longest
Mini batch size	128
Shuffle	'every epoch'
Input size	5

5 Results

The training progress helps us to estimate if the network's accuracy is improving with each epoch. Fig. 2 compares the predicted *Dst* detections (blue) with the actual *Dst* data (red) based on GT-dataset classification. The LSTM model assigns labels to the training data on the basis of GT-dataset. Once the model is implemented, the predicted values are checked against the testing data to know the accuracy of the model. Fig. 3 shows the highest checkpoint accuracy achieved by the model is 83.47% in the 70-80 epoch band. Checkpoints are the weights of the model and allow us to monitor any loss or accuracy during the training process. This implies that the LSTM model was able to accurately detect *Dst* index, and ultimately storm periods with up to 83.47% mean accuracy within a range of $\pm$ 4.35% based on the training data that it was fed with. To test the statistical accuracy of the model with the real-time results of *Dst*, we plot the *Dst* activity for the international disturbed days of 2017. These include the storms of 8 Sep (day 251) , 7 Sep (day 250) and 28 May (day 148) with minimum recorded *Dst* to be -122nT, -68nT and -125nT respectively. Fig. 2 shows the performance of the model on the individually tested storm days. This paper shows the visual performance of the LSTM model for strong storm days only, however, the model has predicted detection for remaining 362 days as well. The occurrence of a CME on day 251 caused an unexpected G-4 class geomagnetic storm during the early

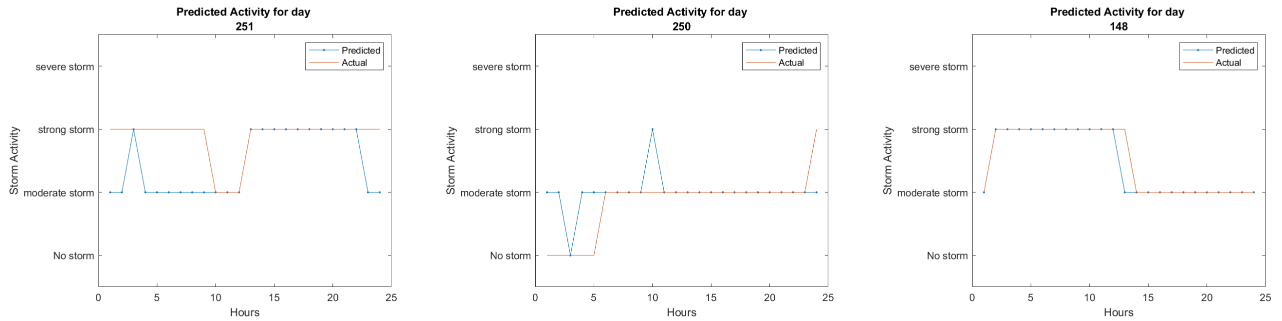

(a) (b) (c)

Figure 2. Dst activity detected by the LSTM model (blue) and the actual Dst activity (red) on storm days (8 Sep, 7 Sep and 28 May)

(00-04) and mid-day (12-18) hours of 8 September 2017 [13]. From 00-03 UT, the K_p value recorded was 7-8+, followed by high speed solar wind, attaining its peak at 1110.1 km/sec at 08/0431Z; *Dst* reaching its minimum of -122 nT at 08/0200Z with *Dst* being consistently $\leq$ -100nT until 08/0600Z. This disturbed period was detected by our model at 0/0200Z and then again at 08/1300Z when *Dst* index started declining again towards -100nT. The model was thus able to detect the second phase of the storm that occurred during the mid-day better than it did the first phase. For the second storm, day 250, the recorded *Dst* was positive for almost all day, except at 07/2300Z, from when it saw a sharp fall making the *Dst* to achieve a minimum of -68nT. The model was able to detect the *Dst* values quite well, except for 07/0300Z and 07/1000Z. At these two instants as well, the prediction was for a stronger storm than actual, i.e. moderate for no storm and strong for moderate storm. On day 148, the model worked quite efficiently in detecting the *Dst* and it only varied by an hour between 28/1200Z-28/1400Z, however with accurate prediction. Overall, the model succeeded in detecting the onsets of negative valued *Dst*. The phases of the storm are detected but in some cases, larger than what it should be. This could be possible because the model overestimated. To avoid overestimation by the network we selected the network to be trained on a set of epoch and hidden units. The details of these are mentioned in Table 3.

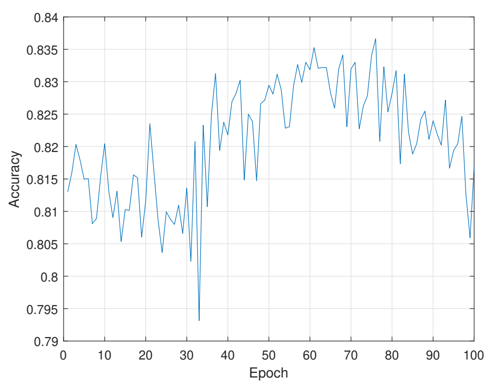

Figure 3. Checkpoint Accuracy

Table 3. Epoch and HU combinations. M1, M2: Max and Min Accuracy with outliers; M3, M4: Max and Min Accuracy without outliers

Epoch	HU	M1	M2	Outliers	M3	M4
250	500	0.8344	0.7969	14	0.8292	0.7969
250	250	0.8342	0.7830	0	0.8342	0.7830
250	100	0.8347	0.2957	5	0.8347	0.8138
250	50	0.8320	0.6473	9	0.832	0.8192
100	500	0.8374	0.7969	0	0.8347	0.7969
100	250	0.8353	0.7917	2	0.8353	0.8090
100	100	0.8347	0.7507	3	0.8347	0.8164
100	50	0.8317	0.4568	7	0.8317	0.8161
30	500	0.8340	0.8008	1	0.8340	0.8122
30	250	0.8288	0.7862	2	0.8288	0.8191
30	100	0.8336	0.6801	3	0.8336	0.8087
30	50	0.8289	0.0574	8	0.8259	0.8047

To ensure that the model delivers with maximum accuracy, we performed several simulations by varying the number of epochs and hidden units per layer. Table 3 lists the results of various trials conducted on the model. For a network to deliver its best results, its important to choose the right number of epochs, as it allows learning algorithm to run until the error from the model has been sufficiently minimized. Using 500 hidden units with 100 epochs in a single layer, making a total of 1400 iterative loops seemed the best fit to train the LSTM model. This implies that the system trained itself 1400 times each time trying to achieve maximum training accuracy and minimum training loss thereby making it the best fit for this problem. This also helped in achieving high detection accuracy of the storm onset, which is the purpose of this study. For each epoch and its corresponding HU, the number of outliers or spikes should be as close to zero as possible. Having outliers signifies the presence of errors in the form of redundant data and it changes the variations and mean of accuracy by a large extent. A combination (100E,500HU) which delivers maximum accuracy with minimum outliers was thus selected. Therefore, before finalising the network, we tested the various possible combinations of LSTM architecture based on their hidden units and epochs to find the model that best predicts Dst with an attainable accuracy of more than 80%. From fig.2, we can infer that the LSTM model was able to detect the moderate storms quite efficiently. From the simulations of the rest of the days, we can also gather that the model accurately detected the weak storms and some instances of upto strong storm.

6 Conclusion and Future Work

In this paper, we presented an LSTM model that that is able to detect the onset of geomagnetic storms based on the Sun's and Earth's magnetic data of previous years with a detection accuracy of more than 83%. The response of the network has been highly correlated with periods of low-moderate geomagnetic activity. Larger batch/epoch sizes make the overall learning process slower by taking epoch*iteration steps but the finally result in a convergence to a more stable model exemplified by lower variance. We can conclude that the model can be used to quite accurately detect low-moderate geomagnetic storms ($Dst \leq$-100nT). It has also predicted strong storm activity (day 251 and day 148) however, it is time lagged. Another possible reason that this model did not detect strong-severe storms might be because of the fact that it was trained with data that had over 170+ minor and hardly 10 severe storms. Since LSTM is known to 'better' remember the previous inputs using the 'memory cell' to be fed to the next state, the network did not have 'enough' occurrences of severe storm to understand and classify it, thus leading it to efficiently detect low-moderate storms. A consistent period of higher solar activity can be further studied to verify the accuracy of this model.

To improvise this network, for detecting storms of $Dst \leq$-200nT, this network can be modelled by more features to the GT-dataset which include the solar and IMF parameters. In order to gain insight into the improved response of this model's behaviour, we have to study train the model with a dataset that includes consistent strong-to-severe storm activity.

Acknowledgment

The solar and geomagnetic data used in this study is available at OMNIWeb, maintained by GSFC, NASA (`https://omniweb.gsfc.nasa.gov/ow.html`). Information about internationally disturbed days and the provisional Dst index is available at WDC, Kyoto (`http://wdc.kugi.kyoto-u.ac.jp/index.html`). Authors acknowledge and thank these data repositories for providing data in open-access.

References

[1] O. S. Oyekola, "Geomagnetic activity index Ap and the occurrence rates of geomagnetic storms during 1996-2017," in *42nd COSPAR Scientific Assembly*, vol. 42, pp. C1.1–47–18, July 2018.

[2] T. Iyemori, H. Maeda, and T. Kamei, "Impulse response of geomagnetic indices to interplanetary magnetic field," *Journal of geomagnetism and geoelectricity*, vol. 31, no. 1, pp. 1–9, 1979.

[3] J.-G. Wu and H. Lundstedt, "Geomagnetic storm predictions from solar wind data with the use of dynamic neural networks," *Journal of Geophysical Research: Space Physics*, vol. 102, no. A7, pp. 14255–14268, 1997.

[4] A. Nagai, *Prediction of magnetospheric parameters using artificial neural networks*. PhD thesis, Rice University, 1994.

[5] R. Bala and P. Reiff, "Improvements in short-term forecasting of geomagnetic activity," *Space Weather*, vol. 10, no. 6, 2012.

[6] J. R. Ayala Solares, H.-L. Wei, R. J. Boynton, S. N. Walker, and S. A. Billings, "Modeling and prediction of global magnetic disturbance in near-earth space: A case study for kp index using narx models," *Space Weather*, vol. 14, no. 10, pp. 899–916, 2016.

[7] J. Lazzús, P. Vega, P. Rojas, and I. Salfate, "Forecasting the dst index using a swarm-optimized neural network," *Space Weather*, vol. 15, no. 8, pp. 1068–1089, 2017.

[8] M. Chandorkar, E. Camporeale, and S. Wing, "Probabilistic forecasting of the disturbance storm time index: An autoregressive gaussian process approach," *Space Weather*, vol. 15, no. 8, pp. 1004–1019, 2017.

[9] M. A. Gruet, M. Chandorkar, A. Sicard, and E. Camporeale, "Multiple-hour-ahead forecast of the dst index using a combination of long short-term memory neural network and gaussian process," *Space Weather*, vol. 16, no. 11, pp. 1882–1896, 2018.

[10] G. Cianchini, A. Piscini, A. De Santis, and S. A. Campuzano, "Fast dst computation by applying deep learning to swarm satellite magnetic data," *Advances in Space Research*, vol. 69, no. 2, pp. 837–855, 2022.

[11] H. Gleisner, H. Lundstedt, and P. Wintoft, "Predicting geomagnetic storms from solar-wind data using time-delay neural networks," in *Annales geophysicae*, vol. 14, p. 679, 1996.

[12] C. Loewe and G. Prölss, "Classification and mean behavior of magnetic storms," *Journal of Geophysical Research: Space Physics*, vol. 102, no. A7, pp. 14209–14213, 1997.

[13] I. Gulati, H. Li, S. Stainton, M. Johnston, and S. Dlay, "Investigation of ionospheric phase scintillation at middle-latitude receiver station," in *2019 International Symposium ELMAR*, pp. 191–194, IEEE, 2019.